

## **The fabrication of p-Ge/n-Si photodetectors, compatible with back-end Si CMOS processing, by low temperature (< 400 °C) molecular beam epitaxy and electron-beam evaporation**

Prabhakar Bandaru, Subal Sahni and Eli Yablonovitch  
Department of Electrical Engineering,  
University of California at Los Angeles, Los Angeles, CA 90095

Hyung-Jun Kim and Ya-Hong Xie  
Department of Materials Science and Engineering,  
University of California at Los Angeles, Los Angeles, CA 90095

### **ABSTRACT**

We report on the low temperature growth, by molecular beam epitaxy (375 °C) and electron-beam evaporation (300 °C), of p-Ge films on n-Si substrates for fabricating p-n junction photodetectors, aimed at the integration of opto-electronic components with back-end Si CMOS processing. Various surface hydrogen and hydrocarbon removal treatments were attempted to improve device properties. We invoke Ge diffusion and growth modes as a function of deposition temperature and rate to correlate structural analysis with the device performance.

### **INTRODUCTION**

Silicon has been the mainstay of the micro-electronics industry, and a very large infrastructure has been built around it, both in terms of the materials research and the capital equipment that is used for fabrication. In recent years, the advent of the Silicon-On-Insulator (SOI) technology, the feasibility of constructing Photonic Integrated Circuits (PICs) and the continuing trend towards miniaturization and multi-functionality has provided impetus for the construction of Silicon based micro-photonics as well. In addition to the practical advantages of a monolithic platform with integrated electronic and optical circuitry for information processing and communication, Si based photonics and opto-electronics offers a way to overcome problems, such as increased power dissipation and reduced speed of operation due to cross-talk, inherent to miniaturization and the consequent scaling down of interconnect density<sup>1</sup>.

We investigate photonic materials, processes and devices that are amenable to integration with existing CMOS (Complementary Metal Oxide Semiconductor) based electronic circuitry. This scheme of integration is preferred as it avoids changes in standard foundry processes, and could lead to easier realization and quicker adoption of optics vis-à-vis electronics. However, such back-end processing is restricted to less than 450 °C to avoid degrading the Al/Ti metallization. A projected application is in fiber based ( $\lambda$ :1.3- 1.55  $\mu\text{m}$ ) communication systems. One could envisage fiber coupling in the optical signals directly onto a substrate, where the light is guided and electronically detected using waveguides and photodetectors respectively. For Si based photonics, the refractive index difference between Si and  $\text{Si}_x\text{N}_y/\text{SiO}_2$  can be used for waveguides, while Germanium on Si could work well as an electronic p-n junction photodetector. Ge is a good choice at 1.55  $\mu\text{m}$  due to a direct band gap of 0.8 eV. (Although, GaAs and InP based semiconductors have higher efficiencies they are excluded from our study due to the difficulty of integration with Si processing) However, the deposition of good quality Ge films on Si once again involves high temperatures<sup>2</sup> for growth and cleaning ( $\sim 800$  °C) and buffer

layers to accommodate the lattice mismatch. Besides the large thermal budget, high temperature processing rules out integrating the growth sequence with a practical back-end fabrication process, and can lead to impurity segregation and diffusion. .

The feasibility of a photo-detector, compatible with back-end CMOS processing, fabricated through low temperature Ge growth ( $< 400\text{ }^{\circ}\text{C}$ ) is the focus of this study. Both electron-beam (e-beam) evaporation and Molecular Beam epitaxy (MBE) were used to grow p-Ge films on n-Si substrates for device fabrication. We attempt to correlate thin film morphology with the electrical response of the photodetector using well known diffusion and growth models.

## EXPERIMENTAL DETAILS

Ge films (100-200 nm thick) were deposited on n-type Silicon substrates ( $\rho$ : 1.5 – 20  $\Omega\text{cm}$ ) by both e-beam evaporation (CHA: base pressure of  $3 \cdot 10^{-6}$  Torr, and Molecular Beam Epitaxy (MBE, Riber EVA 32: base pressure  $8 \cdot 10^{-10}$  Torr). The films were found to be p-doped ( $\rho$ : 0.06-1  $\Omega\text{cm}$ ), as grown. The growth temperature was  $375 \pm 25\text{ }^{\circ}\text{C}$  for MBE and  $300 \pm 10\text{ }^{\circ}\text{C}$  for e-beam evaporation. Prior to deposition, the substrates were cleaned by minor adaptations on the standard Shiraki clean<sup>3</sup> and then treated with a final dip in buffered HF, which removes the surface oxide, passivates the Si, and leads to a hydrogen terminated surface (H-Si) stable in air<sup>4,5</sup>

When a Ge thin film is grown on Si (100), the surface preparation of the Si substrate is critical. The following could affect the quality of low temperature grown Ge films: (1) the large lattice parameter mismatch ( $\sim 4.2\%$ ) with Si; beyond a critical thickness<sup>10</sup>, the strain is normally relieved by misfit dislocations: mid-bandgap deep level defects that contribute to leakage current as carrier recombination centers, (2) the H terminated Si (100) surface<sup>5</sup> (H-Si), which could reduce the Ge adatom mobility and cause non-wetting behavior and island formation, and (3) surface contamination from the ambient, including hydrocarbons. This study explores the extent to which the above factors can be tolerated for low temperature device fabrication. We attempt to remove the H atoms *in situ* by pre-deposition annealing at  $450\text{ }^{\circ}\text{C}$  (Table I). In order to desorb surface hydrocarbons, we adopt two methodologies, *viz.* (1) a  $200\text{ }^{\circ}\text{C}$  pre-bake for 50 minutes, and (2) a stepped temperature increase<sup>6</sup>,  $200\text{ }^{\circ}\text{C} \rightarrow 250\text{ }^{\circ}\text{C} \rightarrow 275\text{ }^{\circ}\text{C}$ , which could also help in reducing the dislocation density at the Si-Ge interface<sup>7</sup>.

The growth of Ge on Si, in MBE, was monitored by Reflection High Energy Electron Diffraction (RHEED). The crystal quality and strain of as-grown Ge/Si structures was probed by *ex situ* x-ray diffraction (both  $\theta$ - $2\theta$  and rocking curves) using  $\text{CuK}\alpha_1$  ( $1.5406\text{ \AA}$ ) radiation in a double-axis Bede3 diffractometer. The electrical and optical properties of both large ( $5\text{ mm} \times 5\text{ mm}$ ) and  $200\text{ }\mu\text{m} \times 200\text{ }\mu\text{m}$  mesa p-n junctions were studied<sup>8</sup>. Ohmic contacts were made on the Si through Ti/Al and on Ge using silver and Au/Pd. The defect density was estimated by counting the etch pits produced by immersing the samples in a diluted Superoxol mixture<sup>9</sup> ( $1\text{ H}_2\text{O}_2$ :  $1\text{ HF}$ :  $55\text{ H}_2\text{O}$ ) for 15 hours. The etch pit density is significantly higher in the e-beam samples ( $2 \cdot 10^{10}\text{ /cm}^2$ ) compared to MBE samples ( $5 \cdot 10^8\text{ /cm}^2$ ). The photo-detector performance, however, is not as adversely affected. While a figure of merit, responsivity (R) is often quoted in literature, it is wavelength and device dependent (e.g. anti-reflection coatings can enhance R) and *a better metric for the quality of the deposited Ge film is the minority carrier (electrons in p-Ge) diffusion length ( $L_n$ )*, which will be reported here.

## EXPERIMENTAL RESULTS AND DISCUSSION

### Electrical Characterization

The Current (I)-Voltage (V) curves of the fabricated p-Ge/n-Si junction photo-detectors were measured *with* and *without* illumination (Figure 1). The photo-current is the net difference. AC measurements using a lock-in amplifier, where the illuminating light (1.3  $\mu\text{m}$ ) was modulated, gave similar values. The minority carrier diffusion lengths ( $L_n$ ) were calculated from the measured photo-responsivity (photocurrent per unit input power) and internal quantum efficiencies<sup>8</sup> and are tabulated along with the leakage/dark current densities ( $J_d$ ) in Table I.

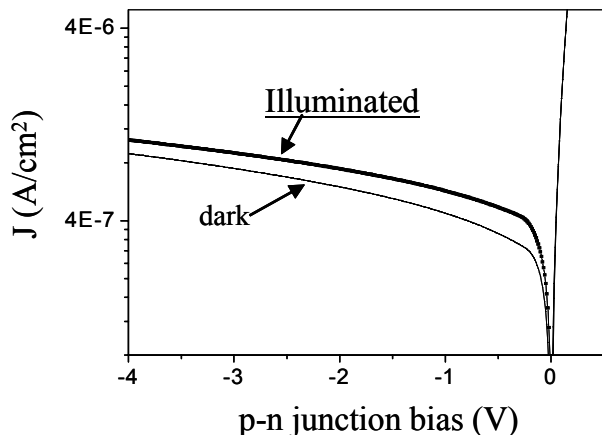


**Figure 1** Electrical characterization of the p-Ge/n-Si photodetector. The difference in the current densities ( $J$ ) as a function of the applied bias ( $V$ ) across the p-n junction *with* and *without/dark* illumination gives the magnitude of the leakage current. The device response and the value of the diffusion length ( $L_n$ ) can be obtained from  $J$  (illuminated).

To assess the effects of the Si substrate preparation, we compare the minority carrier diffusion lengths ( $L_n$ ) of deposited Ge films, to the  $L_n$  ( $\sim 60$  nm) of a film deposited on a Si surface<sup>2</sup> subject to a high temperature oxide (800 °C) desorption treatment. While in excess of the CMOS back-end processing temperature, this control sample still provides a metric. It was seen that appropriate hydrocarbon desorption and hydrogen removal treatments could result in comparable figures of merit, e.g.  $L_n$  of 30 nm in samples MBE 7 and 12 (Table I). We also observe that e-beam samples (i.e., EB1 and EB3) give values of  $L_n$ , and hence responsivity, similar to the MBE grown films which indicates that the diffusion current is the major contributor to the observed photoresponse in either case.

The leakage current densities ( $J_d$ ) are uniformly low in the MBE samples at 0.3 mA/cm<sup>2</sup> while they are up to five times higher (1.5 mA/cm<sup>2</sup>) in the e-beam samples (EB1 and 3). While the small band gap of Ge is an intrinsic cause of leakage currents, the defects at the imperfect Si-Ge interface also contribute in a big way. The leakage currents were modeled by accepted mechanisms<sup>10</sup> of space-charge generation and carrier diffusion where it was seen that the carrier lifetime was indeed limited by interface defect and dislocation induced recombination centers<sup>8</sup>. However, compared to other p-Ge/n-Si diodes from published literature<sup>11</sup>, the much lower leakage current densities in our samples could be primarily due to the slower growth rate of 0.2 Å/sec; this allows the adatoms greater time to diffuse and is necessary to inhibit island formation.

An increase in leakage current density for the e-beam samples could be due to the lower growth temperature, i.e. 300°C (the maximum temperature in our evaporator). If we assume that the activation energy barrier for Ge diffusion to be similar to that calculated for Si on a H-Si<sup>12</sup> surface ( $\sim 5.3$  eV), it is calculated that the diffusion at 300°C is five orders of magnitude lower than that for MBE growth, carried out at 375 °C. The reduced Ge adatom diffusion then enhances island formation, contributing to additional leakage currents.

**Table 1:** Minority carrier diffusion lengths ( $L_n$ ), as a metric of photodetector performance and deposited Ge film quality, were measured in samples grown by Molecular Beam Epitaxy (MBE) and electron- beam evaporation (EB) The figures in parentheses ( ) refer to the measured leakage current densities. ( $L_n$  was computed using  $\alpha: 10^4 \text{ cm}^{-1}$  at 1310 nm,  $J_d$ : leakage current density @ -1V bias, growth temperature: 375 °C, base pressure:  $8 \cdot 10^{-10}$  Torr)

Silicon substrate Surface Preparation	2.45 Å/sec	1.5 Å/sec	1.0 Å/sec	0.5 Å/sec	0.2 Å/sec
Only HF clean	<u>MBE 4</u> $L_n \sim 5 \text{ nm}$ (0.3 mA/cm <sup>2</sup> )	<u>EB 1</u> $L_n \sim 10 \text{ nm}$ (1.6 mA/cm <sup>2</sup> )	<u>MBE 1</u> $L_n \sim 5 \text{ nm}$ (0.1 mA/cm <sup>2</sup> )		<u>MBE 5</u> $L_n \sim 15 \text{ nm}$ (0.6 mA/cm <sup>2</sup> )
HF clean + 450 °C hydrogen desorption (15 mins)					<u>MBE 7</u> $L_n \sim 30 \text{ nm}$ (0.3 mA/cm <sup>2</sup> )
HF clean + 200 °C hydrocarbon desorption (50 mins)				<u>EB 3</u> $L_n \sim 15 \text{ nm}$ (1.8 mA/cm <sup>2</sup> )	<u>MBE 9</u> $L_n \sim 16 \text{ nm}$ (0.3 mA/cm <sup>2</sup> )
HF clean + 450 °C hydrogen desorption + (15 mins) 200 °C hydrocarbon desorption (50 mins)					<u>MBE 12</u> $L_n \sim 30 \text{ nm}$ (0.3 mA/cm <sup>2</sup> )

### Structural Analysis: X-ray Diffraction

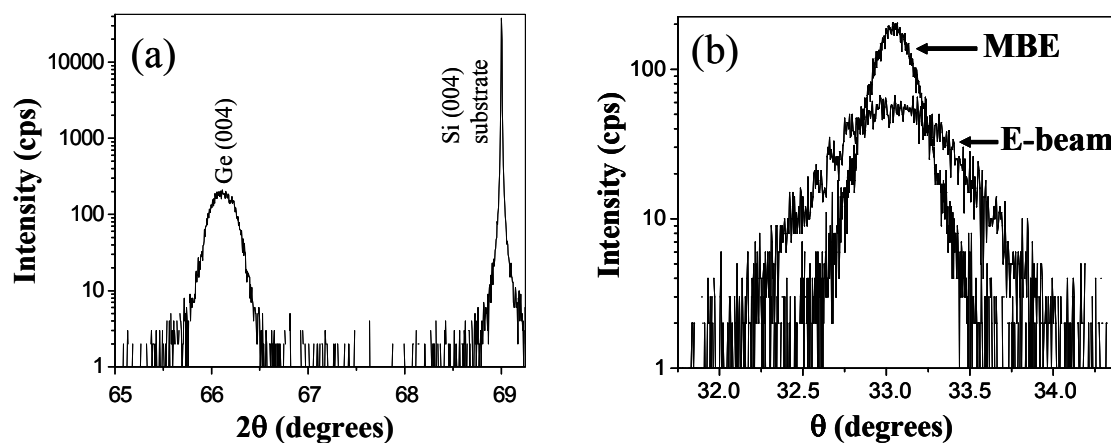


**Figure 2 (a)** X-ray diffraction (XRD) spectrum of the p-Ge – n-Si photodetector structure. The (004) peaks of the Si substrate and the p-Ge film are shown, **(b)** A comparison of the rocking curves in XRD of the MBE and e-beam evaporated films.

Figure 2 illustrates a typical x-ray diffraction spectrum obtained from the Ge-Si samples. The substrate Si (004) was used as a marker for calibrating the  $\theta$ - $2\theta$  scans. A comparison of the

rocking curve widths and peak intensities was used to gauge the crystallinity *vis-à-vis* quality and photoresponse of the deposited Ge. The FWHM values are in the range of  $0.3^\circ - 0.7^\circ$ , a Ge film morphology which is moderately polycrystalline or with low angle grain boundaries is inferred.

### **Low temperature Germanium growth on Silicon**

At near-equilibrium conditions, to accommodate the large lattice mismatch, Ge grows on Si in the Stranski-Krastanov (S-K) mode<sup>13,14</sup>, i.e. a wetting thin film for three mono-layers, followed by island formation. The presence of a uniform Ge film close to the p-n junction interface is beneficial to the junction quality and a large wetting layer thickness is desired. However, deviations from the S-K mechanism are observed<sup>13</sup>, on *non-ideal* surfaces, at low growth temperatures, as also seen in the present study. The following observations were made through RHEED during MBE growth. During the first few monolayers the formation of islands was observed. After 50-70 nm of Ge has been deposited, surface roughness decreased and either a (1 X 1) or (2 X 1) pattern was seen, indicating crystalline Ge growth. At this stage, the effects of the hydrogen and surface roughness are diminished and the film is completely relaxed by the formation of dislocations and other strain relieving defects. (2 X 1) dimers are favored as Ge adatom diffusion along the dimer rows has a lower activation energy (0.64 eV) than that perpendicular to the rows (0.8 eV)<sup>14</sup>. It is speculated that the (2 X 1) reconstruction, seen for example in samples MBE 7 and 12 (Table I) indicate greater extent of Ge adatom diffusion than in the (1 X 1) patterns observed in other samples (e.g. MBE 5), which correlates to higher quality of deposited Ge, greater  $L_n$  and better photodetector performance.

It has been observed<sup>15,16</sup>, from earlier surface science studies, that the H desorption from the Si (100) substrate, especially for the (1 X 1) reconstructed  $\text{SiH}_2$  phase, is a two-step process; the two hydrogen atoms desorb at 420 °C and 520 °C respectively. Since we carry out the hydrogen treatment at 450 °C, the maximum CMOS back-end processing temperature, it is plausible that the surface is only partly depleted of H. The area available for Ge adatom diffusion and the  $L_n$  presumably scale with the amount of H-devoid Si surface.

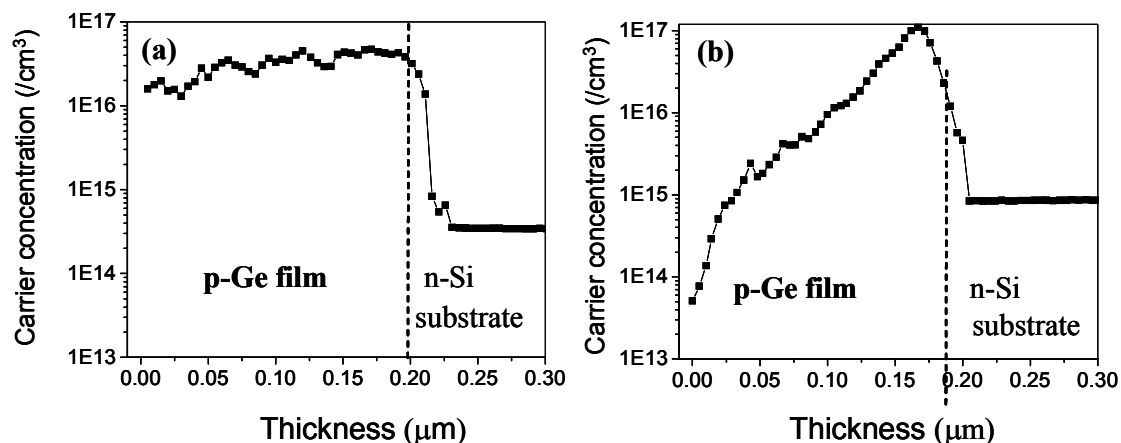


**Figure 3** Spreading Resistance Analysis (SRA) of Ge films deposited by (a) MBE and (b) electron-beam evaporation. The surface of the e-beam evaporated sample is almost intrinsic, whereas in the MBE samples the concentration is more uniform, possibly due to higher substrate surface purity and increased growth temperatures

The reduced diffusion of Ge at the lower growth temperatures could cause the inhomogeneity in the carrier concentration profile. A Spreading Resistance Analysis (SRA) comparison (Figures 3a and 3b) of as grown p-doped (Boron) MBE and e-beam samples (unintentionally doped) shows that the Ge surface is almost intrinsic ( $n_{\text{surface}} \sim 5 \cdot 10^{13} / \text{cm}^3$ ) in the latter. A plausible explanation is that the p-dopants in Ge are not activated at the low growth temperatures; the presence of hole-repelling positive ions (e.g.  $\text{H}^+$ /un-reconstructed Ge atoms) at the surface is also possible. These surface moieties could contribute to the leakage current.

## CONCLUSIONS

We have demonstrated a low temperature grown p-Ge/n-Si photodetector, fabricated by both MBE and electron-beam evaporation, compatible with back-end ( $< 450$  °C) CMOS processing, which could pave the way for Silicon based photonics<sup>8</sup>. In addition to practical electronics-photonics integration, such a study also yields insights into understanding the mechanisms that govern low temperature and non-equilibrium thin film growth. It was seen that a Si substrate surface subject to a combined hydrogen and hydrocarbon desorption treatment gives the best photo-response. The minority carrier diffusion length ( $L_n$ ) in p-Ge seems to scale with the extent to which the hydrogen is removed from the surface.

## ACKNOWLEDGMENTS

We gratefully acknowledge the help of Atif Noori in the x-ray diffraction, the nano-electronics laboratory at UCLA and support from DARPA (MDA972-02-1-0019).

## REFERENCES

1. Fitzgerald, E. A. & Kimmerling, L. C., *MRS Bulletin* **23**, 39 (1998).
2. Watson, G. P., Fitzgerald, E. A., Xie, Y. H. & Monroe, D., *J. Appl. Phys.*, **75**, 263 (1994).
3. Thompson, P. E., Twigg, M. E., Godbey, D. J., Hobart, K. D. & Simons, D. S., *J. Vac. Sci. & Tech. B* **11**, 1077 (1993).
4. Eaglesham, D. J., Higashi, G. S. & Cerullo, M., *Appl. Phys. Lett.* **59**, 685 (1991).
5. Trucks, G. W., Raghavachari, K., Higashi, G. S. & Chabal, Y. J., *Phys. Rev. Lett.* **65**, 504 (1990).
6. Grunthaner, F. J. & Grunthaner, P. J. *Mat. Sci. Reports*, **1**, 65 (1986).
7. Eaglesham, D. J. & Cerullo, M. *Phys. Rev. Lett.*, **64**, 1943 (1990).
8. Bandaru, P. R., Sahni, S., Yablonovitch, E., Kim, H.-J. & Xie, Y.-H., *J. Appl. Phys.* (submitted).
9. Holmes, P. J. in *The Electrochemistry of Semiconductors* (ed. Holmes, P. J.), Academic Press, New York, (1962).
10. Grove, A. S. *Physics & Tech. of Semiconductor Devices*, John Wiley, New York, (1967).
11. Masini, G., Colace, L. & Assanto, G., "*Germanium Thin Films on Silicon for detection of near-infrared light*" (ed. Nalwa, H. S.), Academic Press, New York, (2002).
12. Jeong, S. & Oshiyama, A., *Phys. Rev. Lett.*, **79**, 4425 (1997).
13. Fitzgerald, E. A., *Mat. Sci. Reports* **7**, 87 (1991).
14. LeGoues, F. K., Copel, M. & Tromp, R. M., *Phys. Rev. B*, **42**, 11690 (1990).
15. Frotzheim, H., Kohler, U. & Lammerling, H., *Surf. Sci.*, **149**, 537 (1985).
16. Thanh, V. L., Bouchier, D. & Hncelin, G., *J. Appl. Phys.*, **87**, 3700 (2000).